Fiber Connectivity Density Mapping in End-stage Renal Disease Patients: A Preliminary Study

Chi Ma
The Affiliated Hospital of Qingdao University
Xinghai Jiang
Centers for Disease Control and Prevention
Yande Ren (8198458@163.com)
The Affiliated Hospital of Qingdao University https://orcid.org/0000-0002-8737-3461
Gaojie Gu
Shandong University of Science and Technology
Airong Fu
Qingdao west coast new district central hospital
Chengjian Wang
The Affiliated Hospital of Qingdao University
Peirui Bai
Shandong University of Science and Technology
Tong Zhou
The Affiliated Hospital of Qingdao University
Shanshan Qin
The Affiliated Hospital of Qingdao University
Shengli Fu
The Affiliated Hospital of Qingdao University

Research Article

Keywords: end-stage renal disease, diffusion tensor imaging, fiber connectivity map, structural connectivity, cognitive impairment

Posted Date: February 15th, 2021

DOI: https://doi.org/10.21203/rs.3.rs-204848/v1

Version of Record: A version of this preprint was published at Brain Imaging and Behavior on January 9th, 2022. See the published version at https://doi.org/10.1007/s11682-021-00604-7.

Abstract

Abnormal brain structural connectivity of end-stage renal disease (ESRD) is associated with cognitive impairment. However, the characteristics of cortical structural connectivity have not been investigated in ESRD patients. The current study aimed to investigate the structural connectivity of the entire cerebral cortex in ESRD patients. Twenty-five ESRD patients and 20 healthy controls were recruited for this study; all participants underwent diffusion tensor imaging and high-resolution T1-weighted imaging scanning. Fiber connectivity density (FiCD) mapping was performed to calculate structural connectivity of the whole cortex, and between-group differences were compared in a vertexwise manner. We also tested the associations between FiCD changes and clinical information using Pearson correlation analysis. The results demonstrated that the mean global FiCD value was significantly decreased in ESRD patients compared with that of HCs. Notably, FiCD values were significantly changed (decreased or increased) in certain cortical regions, which mainly involved the bilateral dorsolateral prefrontal cortex (DLPFC), inferior parietal, lateral temporal and middle occipital cortex ($P < 0.01$ with Monte Carlo correction). Moreover, in ESRD patients, the increased FiCD values in the right middle frontal gyrus were negatively correlated with serum creatinine ($r=-0.473$, $p = 0.017$) and urea levels ($r=-0.511$, $p = 0.009$). The increased FiCD values in the left middle frontal gyrus were negatively correlated with dialysis duration ($r=-0.577$, $p = 0.003$) and parathyroid hormone (PTH) levels ($r=-0.552$, $p = 0.004$). Our results suggested that ESRD patients exhibited extensive impaired cortical structural connectivity. And there may be a compensation mechanism of cortical structural recombination that plays a role in the way the brain adapts to maintain optimal network function. Moreover, serum creatinine, urea and PTH levels may be risk factors for brain structural network decompensation in ESRD patients.

1. Introduction

Patients with end-stage renal disease (ESRD) are known to have a higher prevalence of cognitive impairment(Drew et al., 2019). Studies have shown that even younger dialysis patients have severe overall cognitive impairment and that all age groups receiving dialysis have poorer cognitive function than their peers(Chu & McAdams-DeMarco, 2019). The development of cognitive impairment in ESRD patients was thought to be multifactorial. ESRD usually coexists with multiple comorbidities. Arteriosclerosis, hypertension and hyperlipidemia are pathophysiological continuums that occur in chronic kidney disease (CKD) and gradually increase as renal function declines(Georgianos et al., 2018). CKD has been identified as an independent risk factor for cerebrovascular disease, particularly small-vessel cerebrovascular disease, which can lead to cognitive dysfunction(Yamamoto et al., 2011). Next, anemia(Kurella et al., 2011) and secondary hyperparathyroidism(Lourida et al., 2015) were also thought to be associated with cognitive impairment and dementia. Another noteworthy factor is dialysis, which may indirectly affect cognition as it can lead to rapid fluid transfer and swings in blood pressure(Daugirdas, 2001; Eldehni & McIntyre, 2012).

The underlying neuropathologic processes of cognitive impairment in ESRD patients are complex and remain unclear. Functional neuroimaging evidence has shown characteristic patterns of disconnection

between intrinsic brain networks of functionally related but spatially separated brain regions; in particular, the default mode network (DMN) has been implicated in ESRD patients, suggesting that the cognitive and behavioral disturbances of ESRD are an expression of the inability of the brain to achieve functional integration(Lu et al., 2019; Ni et al., 2014). However, the shortcoming of functional neuroimaging studies is that they cannot determine whether these abnormal connections are caused by abnormal white matter (WM) fiber pathways or by aberrant synaptic transmission in cortical areas.

Traditional MRI studies have shown that the risk of ischemic WM disease in patients with CKD is higher than that in the general population, and mainly manifests as confluent WM hyperintensity (WMH) and subcortical lacunar infarcts(Ağildere et al., 2001). Moreover, the vast majority of diffusion tensor imaging (DTI) studies investigating ESRD have consistently demonstrated that reduced WM integrity and disruptions of brain structural connection networks were intimately associated with neurological complications in ESRD patients(Drew et al., 2017; Eldehni et al., 2019; Mu et al., 2018; Yin et al., 2018). These results seem to indicate that there is a “disconnection” of WM fiber pathways, which may provide the anatomical basis for abnormal brain functional interactions.

Despite promising results revealing WM abnormalities in ESRD patients, current DTI studies have major shortcomings. A major limitation of these studies is the inability to provide a direct and comprehensive analysis of the structural connectivity of the whole cortex. For example, both region of interest (ROI) and diffusion tensor tractography (DTT) methods have low reproducibility, as the reproducibility is dependent on the location and size of the ROI selected by the researcher. Similarly, the results of graph analysis methods are limited by the selection of prior templates. Next, it is inherently difficult to measure the structure connectivity corresponding to the cerebral cortex using the tract-based spatial statistics (TBSS) method. Moreover, the mean fractional anisotropy (FA) for most DTI studies in quantitative comparisons that characterize structural connectivity is a good measure of fiber integrity, but it is not the best indicator to measure the strength of anatomical connectivity between two brain regions, mainly because it does not account for the number of fibers or ROI size(Huang & Ding, 2016).

A recent technique combining a diffusion tractography technique and cortical surface-based analysis, named fiber connectivity density (FiCD) mapping(Liu et al., 2017), can measure the structural connectivity of the whole cortex, which makes it possible to accurately locate the pathologically disconnected areas of the cortex(Liu et al., 2016). Specifically, in the FiCD method, vertexwise multiple statistical analyses is used to compare the whole-cortex connectivity between groups. This data-driven approach can automatically identify brain regions with significant differences at the whole-brain level without the need to define ROIs. Second, the generated FiCD maps were precisely matched into the common brain surface, allowing the WM abnormalities to be located precisely in the cortex. Finally, the FiCD values simultaneously take fiber numbers, the FA values and the size of the corresponding cortical unit into consideration, which may be a more suitable indicator to measure structural connectivity strength and would likely provide more pathophysiological information that can lead to a better understanding the mechanisms of cognitive impairment in ESRD patients.

In this study, we described the first application of FiCD mapping to a cohort of participants clinically diagnosed with ESRD. The aim of this study was to explore the underlying structural connectivity across the entire cerebral cortex in ESRD patients. We additionally investigated whether there were associations between these abnormal cortical connectivities and the clinical variables in patients with ESRD.

2. Materials And Methods

2.1 Participants

The study was approved by the Medical Ethics Committee of the Affiliated Hospital of Medical College of Qingdao University, China, and informed consent was obtained from all participants. All procedures involving human participants conformed to the 1964 Declaration of Helsinki and subsequent revisions or similar ethical standards. For this hospital-based prospective case-control study, 30 ESRD patients who were diagnosed with renal failure, defined by a glomerular filtration rate (GFR) less than 15 mL/min/1.73 m^2, and who underwent regular hemodialysis were recruited from the nephrology and renal transplantation department at our hospital between January 2019 and January 2020. Concurrently, 20 healthy, age- and sex-matched volunteers were recruited from the local community. To avoid possible coupling effects, all subjects in the present study were right-handed and aged between 20 and 50 years. The demographic and clinical data of each ESRD patient were acquired from the electronic medical records in our hospital. All ESRD patients completed a laboratory examination within 24 hours before MR imaging, which included serum creatinine level, urea level, hemoglobin level, hematocrit level, cholesterol and triglyceride level, serum potassium, serum sodium, serum calcium and parathyroid hormone (PTH) level evaluations. All the subjects completed a questionnaire from the Mini-Mental State Examination (MMSE) before MR imaging.

The shared exclusion criteria for patients and control subjects were as follows: (a) history of severe head injury or obvious brain lesions (including WMHs) on T2-fluid-attenuated inversion recovery (FLAIR) images; (b) neurodegenerative diseases (e.g., epilepsy, Parkinson's disease, or Alzheimer's disease); (c) acute cerebrovascular disease or peripheral arterial occlusion; (d) chronic liver failure or heart failure; (e) a history of psychiatric disorders in any control subject or history of major psychiatric disorders in any subject; (f) severe metabolic diseases (e.g., primary hyperparathyroidism or diabetes); (g) substance abuse, including drugs, alcohol or cigarettes; (h) pregnancy or lactation at the time of the study; and (i) contraindications to MRI. Three patients with ESRD were excluded because of obvious WMH lesions, and two patients were excluded because of lacunar infarction. The final study population included 25 patients with ESRD and 20 healthy controls (HCs). Out of the 25 patients with ESRD, 15 (60%) also had renovascular hypertension, 10 (40%) had hyperlipidemia, 18 (72%) had anemia, and 24 (96%) had high PTH levels.

2.2 MR data acquisition

MRI examinations were performed on all subjects using a GE 3T MRI scanner (GE Medical Systems, Milwaukee, WI) equipped with a standard 8-channel head coil. Conventional imaging sequences, which

included T1-weighted images and T2-FLAIR images, were acquired for each subject to detect clinically asymptomatic organic lesions. Subsequently, three-dimensional brain high-resolution T1-weighted structural images were acquired using a 3D magnetization-prepared rapid-acquisition gradient-echo (3D-MPRAGE sequence) with the following parameters: repetition time (TR) = 5.6 ms, echo time (TE) = 1.7 ms, flip angle(FA) = 15°,matrix = 256×256, field of view (FOV) = 25.6 cm × 25.6 cm, and thickness/gap = 1.2/0 mm. This session lasted for approximately 5 min and 15 sec. DTI images were obtained using a single-shot echo-planar imaging (EPI) sequence with 64 diffusion gradient directions (b = 1000 s/mm^2 along 64 non-collinear directions) and a reference image (b = 0 s/mm2). The parameters were as follows: TR = 8700 ms, TE = 70.8 ms, thickness/gap = 3/0 mm, FOV = 24 cm × 24 cm, matrix = 128×128. Each scan lasted approximately 9 min and 16 sec.

2.3 Data preprocessing

First, a the gray matter–white matter(GM-WM) interface of the whole cortex was constructed for each subject based on 3D-T1WI using the FreeSurfer software package(Fischl, 2012) (Version 5.3.0, http://surfer.nmr.mgh.harvard.edu/), by performing the following steps (Fig. 1): correction of uneven fields, removal of nonbrain tissue, automated Talairach transformation, subcortical WM and deep GM segmentation(Fischl et al., 2002), tessellation of the GM-WM boundary, automated topology correction(Segonne et al., 2007), and surface deformation(Dale et al., 1999); these steps were performed according to the intensity gradients to optimally place the GM/WM and GM/cerebrospinal fluid boundaries at the greatest changes in intensity, thus defining transitions to other tissue classes. Second, the diffusion images were corrected for head movement and eddy current, and the brain tissue was extracted using the FSL toolbox(Jenkinson et al., 2012) (Fig. 1).

2.4 FiCD mapping

By combination of a diffusion tractography technique and cortical surface-based analysis, “FiCD mapping” is based on a set of internal algorithms developed by Liu et al(Liu et al., 2017). to measure the structural connectivity of the entire cortex, which has been shown to have good intra- and interindividual reproducibility and can accurately reflect the involved cortical regions. First, the GM-WM interface obtained in the preprocessing step was divided into 2000 cortical units (CUs) using the k-medoids algorithm. Second, the GM-WM interface of the same subject was matched to the diffusion space using the ANTs toolbox. Third, fiber tracking constructions of the whole brain were performed in tractography space by using a deterministic fiber tracking algorithm(Yeh et al., 2013) in DSI Studio with each CU as a seed(Yeh et al., 2010; Yeh & Tseng, 2011). The parameters were set as: FA threshold = 0.14, turning angle threshold = 45°, step size = 0.5, smoothing = 0.5, seed number = 1/voxel, fiber length = 30–300 mm. Fourth, FiCD values of each CU were calculated to construct the whole cortical FiCD map, which was defined as the sum of the mean FA values of the association fibers generated by a CU and then divided by the volume of this CU. According to the research of Liu et al.(Liu et al., 2017), the calculation formula can be expressed as$\mathrm{FiCD}=\frac{\sum_{\mathrm{i}=1}^{\mathrm{n}} FA_{mean}}{\mathrm{V_{cu}}}$, where n represents the total number of association fibers connected to

a single CU, FA_{mean} is the mean fractional anisotropy value, and V_{cu} is the volume of a single CU. Therefore, FiCD values were calculated for 2000 CU of the whole brain and assigned to the corresponding CU, and then the FiCD map of the whole brain of all subjects obtained was spatially normalized to a standard common brain surface(Fischl et al., 1999) through nonlinear registration and smoothed with an isotropic Gaussian kernel with a full width at half-maximum of 10 mm to reduce noise. To improve the normality before statistical analysis between groups, the Z transformation of the FiCD for each vertex was performed, i.e., values were subtracted from the mean and divided by the standard deviation of FiCD for the entire hemisphere.

2.5 Statistical analysis

2.5.1 Group-level comparison of FiCD maps

To identify regions with significant differences between the two groups, vertexwise statistical comparisons of the FiCD value of the common brain surface between groups were performed using the General Linear Model of Query Design Estimate Contrast (Qdec) module in the FreeSurfer software package. Statistical significance was set to $p < 0.01$ (Monte Carlo Null-Z simulation for multiple comparison correction with 10000 iterations). The mean global FiCD values of the two groups were subsequently extracted, and the differences between the groups were compared using a two-sample t test in SPSS 22.0 software with a significance threshold of $p < 0.05$.

2.5.2 Group differences in demographic and clinical data

The differences in demographic and clinical data between the two groups were compared using two-sample t tests and χ^2 tests in SPSS 22.0 software (SPSS Inc., Chicago, IL, USA). Statistical significance was set to $p < 0.05$.

2.5.3 Correlation analyses

A Pearson correlation analysis was used to assess the relationships between FiCD values (after Z transformation) and clinical variables (MMSE scores, dialysis duration, serum creatinine level, urea level, hemoglobin level, hematocrit level, cholesterol and triglyceride level, serum potassium, serum sodium, serum calcium and PTH level) in the ESRD patients.

3. Results

3.1 Demographic and clinical information of the participants

The demographic and clinical information of all patients and healthy subjects are shown in Table 1. There were no significant differences in age, sex or education level between the two groups ($P > 0.05$). The ESRD group had significantly lower MMSE scores than the healthy controls (HCs) ($P < 0.001$).

Table 1
Demographic and Clinical Data of the two Study Groups

Variable	ESRD patients(n = 25)	Healthy controls(n = 20)	T values	P value
Age (years)	38.8 ± 9.7(18–50)	38.4 ± 8.1(24–50)	0.162	0.872[b]
Sex (male/female)	14/11	11/9	0.004	0.947[a]
Education (years)	11.1 ± 3.0(6–16)	11.2 ± 3.5(6–16)	-0.123	0.903[b]
MMSE	28.3 ± 1.1(27–30)	29.8 ± 0.5(28–30)	-5.662	0.000[b]
mean global FiCD	5347.9 ± 214.7	5515.9 ± 159.2	-2.914	0.006[b]
Dialysis duration (month)	9.3 ± 7.9	-		-
creatinine (μmol/L)	713.6 ± 360.1	-		-
Urea (mmol/L)	18.5 ± 9.7	-		-
Ca^{2+} (mmol/L)	2.1 ± 0.2	-		-
K^{+} (mmol/L)	4.4 ± 0.6	-		-
Na^{+} (mmo/L)	139.8 ± 2.8	-		-
Hemoglobin (g/L)	98.7 ± 20.6	-		-
Hematocrit	31.2 ± 6.8	-		-
Cholesterol (mmol/L)	4.4 ± 1.9	-		-
Triglyceride(mmol/L)	2.2 ± 1.9	-		-
PTH (pg/mL)	289.8 ± 192.5	-		-
Values are represented as the mean ± SD. ESRD, end-stage renal disease. PTH: parathyroid hormone.				
a The P-value was obtained by chi-square test.				
b The P-value was obtained by two-sided two-sample t test.				

3.2 Group differences in fiber connectivity density

The mean global FiCD value was significantly deceased in ESRD patients compared with HCs ($p < 0.05$) (Table 1).The vertexwise intergroup comparison showed the FiCD values of the bilateral dorsolateral prefrontal cortex[(DLPFC), including the bilateral middle and inferior frontal gyrus], inferior parietal, lateral middle temporal, and right middle occipital cortex were significantly decreased in ESRD patients, whereas some regions in the bilateral DLPFC (including the bilateral middle and right inferior frontal gyrus), lateral temporal (including the bilateral superior and right middle temporal gyrus), and left middle occipital

cortex of the ESRD group showed significantly increased FiCD values compared to those of HCs (P < 0.01 with Monte Carlo correction) (Table 2; Fig. 2).

Table 2
Regions showing significant differences in FiCD mapping between the ESRD group and the HC group.

	Anatomic regions		Side	Brodmann area	MNI Coordinates (mm)		
					X	Y	Z
ESRD vs. HCs (Monte Carlo Null-Z simulation for multiple comparison correction with 10000 iterations, P < 0.01)							
ESRD < HCs	Dorsolateral prefrontal cortex (DLPFC)	Middle frontal gyrus	L/R	46	45	50	14
		Inferior frontal gyrus	L/R	45	49	28	21
	Inferior parietal cortex		L/R	40	-43	-55	39
	Lateral middle temporal cortex		L/R	21,38	62	-22	-11
	Middle occipital cortex		R	39	45	-79	15
ESRD > HCs	Dorsolateral prefrontal cortex (DLPFC)	Middle frontal gyrus	L/R	46	46	57	-5
		Inferior frontal gyrus	R	47	46	47	-10
	Lateral temporal cortex	Superior temporal gyrus	L/R	22	-53	-4	-5
		Middle temporal gyrus	R	21	55	-40	1
	Middle occipital cortex		L	39	-44	-78	22

3.3 Correlation between functional connectivity and clinical variables

For ESRD patients, the increased FiCD values in the right middle frontal gyrus were negatively correlated with serum creatinine (r=-0.473, p = 0.017) and urea levels (r=-0.511, p = 0.009). The increased FiCD values in the left middle frontal gyrus were negatively correlated with dialysis duration (r=-0.552, p = 0.004) and PTH levels (r=-0.577, p = 0.003) (Fig. 3). There were no significant correlations between FiCD values and other clinical variables (P > 0.05).

4. Discussion

In this study, we used an integrative framework combination of a diffusion tractography technique and cortical surface-based analysis, namely, FiCD mapping, to study the whole cortical structural connectivity in ESRD patients and found that this method can be helpful for characterizing microstructural changes that accompany ESRD patients from the unique perspective of GM-WM integration.

The results showed that the mean global FiCD values of ESRD patients were significantly lower than those of the HCs, suggesting extensive disconnection of the brain cortex in ESRD patients. Second, vertexwise statistical comparisons showed that FiCD connecting the bilateral DLPFC, inferior parietal, lateral temporal and middle occipital cortex were significantly changed (increased or decreased), possibly suggesting regional reconstruction of the brain structural network to adapt to injury.

4.1 Impaired cortical structural connectivity in ESRD patients

Prominent decreased FiCD values were observed in the bilateral DLPFC (including in the bilateral middle and inferior frontal gyrus), bilateral inferior parietal, lateral middle temporal, and right middle occipital cortex, which may be imaging signs of the development of cognitive impairment in ESRD patients. In fact, many previous investigators have demonstrated that ESRD patients had functional and structural abnormalities in the frontal, parietal, temporal, and occipital regions (i.e., decreased functional connectivity(Zheng et al., 2014), cortical thinning(Chiu et al., 2019) and decreased cerebral blood flow(Cheng et al., 2019)) with cognitive decline during the clinically asymptomatic phase. Decreased WM integrity has also been reported in the DTI literature(Chou et al., 2013; Drew et al., 2017), primarily in the fornix, anterior limb of the internal capsule, corona radiata, and anterior thalamic radiation, all of which have extensive anatomical connections with these four regions. In contrast to these studies, we provide a unique and appropriate basis for the integration of GM and WM results, as the two metrics can be accurately matched in a unified space by using FiCD mapping in the present study.

Both the current study and previous studies did not show a clear or consistent pattern in a particular region of ESRD patients. However, evidence highlights the role of the prefrontal cortex (PFC). Anatomically and functionally, the PFC area has a unique but overlapping pattern of connections with almost all sensory neocortex and motor systems and a wide range of subcortical structures, which may allow it to exert a “top-down” influence on a wide range of brain processes(Dixon, 2015). Mechanistically, cognitive impairment is largely secondary to the increased prevalence of cerebrovascular disease, particularly small-vessel cerebrovascular disease in ESRD patients(Krishnan & Kiernan, 2009). Extensive structural disconnection in the prefrontal region has been shown to be a characteristic pattern in small-vessel disease patients with mild cognitive impairment(Liu et al., 2020). Although cognitive impairment in ESRD patients is affected by a variety of comorbidities, the contribution of cerebral vascular diseases seemed to be further supported by the impaired structural connectivity in the DLPFC in our study.

4.2 Pathophysiological significance

By localizing connectivity impairments in ESRD patients to specific cortical regions, our findings provide support for a structural basis for these previous studies. The FiCD value enables estimation of both the axonal density of all associated fibers connected to a CU and the FA value of each associated fiber. Thus, the decrease in FiCD value may be the result of loss of axons leading to atrophy of a fiber bundle across its entire cross-section of a CU(Mito et al., 2018). Another likely scenario is that reduced integrity of the WM is associated with decreased FA values.(Alexander et al., 2007) This may be related to axons degeneration and WM demyelination. On one hand, atrophy of a fiber bundle may mean a reduction in the space occupied by fiber bundles, leading to changes in macroscopic structure and morphology, such as decreased cortical thickness and GM volume(Mito et al., 2018). On the other hand, the speed and capacity of information transmission between a pair of cortical regions connected by a damaged fiber bundle may be reduced. In particular, a reduction in axon density may mean that fewer nerve impulses are transmitted and therefore carry less information, whereas demyelination leads to slower nerve impulses and therefore less speed transmission(RUSHTON, 1951; Zalesky et al., 2011). Thus, the cortical regions exhibiting decreased FiCD values may lead to decreased disconnected functional connectivity due to abnormal WM fiber pathways.

Notably, the decrease in functional connectivity of local cortical regions cannot be fully explained by the interruption of structural connections. The decline in functional connectivity can be ascribed to the destruction of specific WM fibers, neuronal dysfunction, or a combination of the two(Daskalakis et al., 2008; Hagmann et al., 2008). Some regions, such as the medial frontal areas, posterior cingulate cortex, and precuneus, were not identified as showing strong connectivity differences in our study, despite often showing functional reductions in patients. This divergence might reflect the fact that our analysis addresses a unique aspect of neuropathology; that is, connectivity was addressed rather than function. Although the present study was influenced by these limitations, future work will benefit from studying the effects of other pathological injuries in this clinical group.

4.3 Compensation mechanism of structural reorganization

Compared to HCs, the regions of increased structural connectivity described in ESRD patients may suggest a compensating mechanism of structural recombination in the brain that counteracts the damage that occurs in the early stages of chronic progressive disease. Several studies have demonstrated that the increases in brain structure properties can be linked to maintenance of function despite aging or continuous damage, as shown in neurodegenerative disorders(Meunier et al., 2014; Meunier et al., 2010). Similar results were found in previous studies, and notably increased local efficiency but decreased global efficiency in the modular structure of functional networks has been recently demonstrated in ESRD patients using functional MRI (fMRI)(Ma et al., 2015), indicating a disruption and reorganization in the normal balance of functional brain networks in ESRD patients. In a DTI study, a significantly increased node-clustering coefficient was found in ESRD patients(Chou et al., 2019). A higher clustering coefficient indicated high efficiency of information transfer for specialized processing, suggesting that the brain was likely to have increased the structural connectivity of local nodes to maintain transmission efficiency. Thus, these results highlight that the observed changes in

network structural connectivity are not only a result of diffuse brain injury but should be considered an adaptive process for the brain to maintain optimal network function.

In this study, increased FiCD values in the bilateral middle frontal gyrus were negatively correlated with dialysis duration and serum creatinine, urea and PTH levels, suggesting that compensation mechanisms for cerebral structural networks may be exhausted with the progression of the disease. Meanwhile, serum creatinine, urea and PTH levels may be important risk factors for cognitive impairment in ESRD patients. Hence, there is therefore a need for early interventions to prevent disease progression.

4.4 Limitations

Other limitations of the current study should be noted. First, a small sample size leads to a lack of statistical power; thus, the findings need to be confirmed in larger studies. Second, the results of the FiCD mapping method are strongly dependent on the algorithm and parameter settings; these factors are adjustable. A major limitation of the deterministic fiber tracking algorithm used in this study is that the method is particularly hampered by voxels that contain multiple fiber orientations (such as crossing, bending, or fan-shaped fibers)(Mori & van Zijl, 2002). These voxels are difficult to interpret or assign to specific fiber pathways, thus, inaccurate results may have been obtained. Third, some comorbidities associated with ESRD (such as anemia, hypertension, and hyperlipidemia) were not excluded in this study. ESRD cognitive impairment may be a common result of these comorbidities; therefore, it is not necessary to make a strict distinction. Fourth, the study had a cross-sectional design; future work should include longitudinal studies to address how the brain networks adaptively reorganize to compensate for their impaired structural networks. Finally, these correlations between abnormal functional connectivity correlations and clinical variables did not survive stringent correction; thus, they were considered exploratory and need to be validated in a larger sample size.

5. Conclusion

In summary, ESRD patients had extensive cortical structural connectivity impairment, which may be imaging signs for the development of cognitive impairment in ESRD patients. Moreover, there may be a compensation mechanism of cortical structural recombination that plays a role in the way the brain adapts to maintain optimal network function in ESRD patients. In addition, serum creatinine, urea and PTH levels may be risk factors for brain structural network decompensation in ESRD patients. Our study provided novel insight and more pathophysiological information to improve the present understanding the mechanism of ESRD-related cognitive impairment.

Declarations

6. Conflicts of interest

All authors declare that they have no conflict of interest.

7. Authors' contributions

Author contributions included conception and study design (MC JXH and RYD), data collection or acquisition (MC, WCJ and ZT), statistical analysis (MC and GGJ), interpretation of results (MC, JXH,FAR,GGJ, BPR, QSS, FSL and RYD), drafting the manuscript work or revising it critically for important intellectual content (MC, RYD) and approval of final version to be published and agreement to be accountable for the integrity and accuracy of all aspects of the work (All authors).

8. Funding

This work was supported by the Medical and Health Science and Technology Development Program of Shandong Province(2016WS0285).

9. Ethics approval

The study was approved by the Medical Research Ethics Committee of the Affiliated Hospital of Medical College of Qingdao University, China. All procedures performed in studies involving human participants were in accordance with the ethical standards of the institutional and/or national research committee and with the 1964 Helsinki declaration and its later amendments or comparable ethical standards

10. Consent to participate

The patients/participants provided their written informed consent to participate in this study.

References

1. Ağildere, A. M., Kurt, A., Yildirim, T., Benli, S., & Altinörs, N. (2001). MRI of neurologic complications in end-stage renal failure patients on hemodialysis: pictorial review [Journal Article; Review]. *EUROPEAN RADIOLOGY, 11*(6), 1063–1069. http://doi.org/10.1007/s003300000688.
2. Alexander, A. L., Lee, J. E., Lazar, M., & Field, A. S. (2007). Diffusion tensor imaging of the brain [Journal Article; Research Support, N. I. H. Extramural; Research Support, Non-U.S. Gov't; Review]. Neurotherapeutics, 4(3), 316–329. http://doi.org/10.1016/j.nurt.2007.05.011.
3. Cheng, B. C., Chen, P. C., Chen, P. C., Lu, C. H., Huang, Y. C., Chou, K. H., Li, S. H., Lin, A. N., & Lin, W. C. (2019). Decreased cerebral blood flow and improved cognitive function in patients with end-stage renal disease after peritoneal dialysis: An arterial spin-labelling study [Journal Article]. *EUROPEAN RADIOLOGY, 29*(3), 1415–1424. http://doi.org/10.1007/s00330-018-5675-9.
4. Chiu, Y. L., Tsai, H. H., Lai, Y. J., Tseng, H. Y., Wu, Y. W., Peng, Y. S., Chiu, C. M., & Chuang, Y. F. (2019). Cognitive impairment in patients with end-stage renal disease: Accelerated brain aging? [Journal

Article]. *JOURNAL OF THE FORMOSAN MEDICAL ASSOCIATION, 118*(5), 867–875. http://doi.org/10.1016/j.jfma.2019.01.011.

5. Chou, M. C., Hsieh, T. J., Lin, Y. L., Hsieh, Y. T., Li, W. Z., Chang, J. M., Ko, C. H., Kao, E. F., Jaw, T. S., & Liu, G. C. (2013). Widespread white matter alterations in patients with end-stage renal disease: a voxelwise diffusion tensor imaging study [Controlled Clinical Trial; Journal Article; Research Support, Non-U.S. Gov't]. *AJNR Am J Neuroradiol, 34*(10), 1945–1951. http://doi.org/10.3174/ajnr.A3511.
6. Chou, M. C., Ko, C. H., Chang, J. M., & Hsieh, T. J. (2019). Disruptions of brain structural network in end-stage renal disease patients with long-term hemodialysis and normal-appearing brain tissues [Journal Article]. *J Neuroradiol, 46*(4), 256–262. http://doi.org/10.1016/j.neurad.2018.04.004.
7. Chu, N. M., & McAdams-DeMarco, M. A. (2019). Exercise and cognitive function in patients with end-stage kidney disease. *SEMINARS IN DIALYSIS, 32*(4SI), 283–290. http://doi.org/10.1111/sdi.12804.
8. Dale, A. M., Fischl, B., & Sereno, M. I. (1999). Cortical surface-based analysis - I. Segmentation and surface reconstruction. *NEUROIMAGE, 9*(2), 179–194. http://doi.org/10.1006/nimg.1998.0395.
9. Daskalakis, Z. J., Christensen, B. K., Fitzgerald, P. B., & Chen, R. (2008). Dysfunctional neural plasticity in patients with schizophrenia [Journal Article; Research Support, Non-U.S. Gov't]. *Arch Gen Psychiatry, 65*(4), 378–385. http://doi.org/10.1001/archpsyc.65.4.378.
10. Daugirdas, J. T. (2001). Pathophysiology of dialysis hypotension: an update [Journal Article; Review]. *AMERICAN JOURNAL OF KIDNEY DISEASES, 38*(4 Suppl 4), S11–S17. http://doi.org/10.1053/ajkd.2001.28090.
11. Dixon, M. L. (2015). Cognitive control, emotional value, and the lateral prefrontal cortex. Frontiers in Psychology, 6(758) http://doi.org/10.3389/fpsyg.2015.00758.
12. Drew, D. A., Koo, B. B., Bhadelia, R., Weiner, D. E., Duncan, S., la Garza, M. M., Gupta, A., Tighiouart, H., Scott, T., & Sarnak, M. J. (2017). White matter damage in maintenance hemodialysis patients: a diffusion tensor imaging study [Journal Article]. *BMC Nephrology, 18*(1), 213. http://doi.org/10.1186/s12882-017-0628-0.
13. Drew, D. A., Weiner, D. E., & Sarnak, M. J. (2019). Cognitive Impairment in CKD: Pathophysiology, Management, and Prevention [Journal Article; Review]. *AMERICAN JOURNAL OF KIDNEY DISEASES, 74*(6), 782–790. http://doi.org/10.1053/j.ajkd.2019.05.017.
14. Eldehni, M. T., Odudu, A., & Mcintyre, C. W. (2019). Brain white matter microstructure in end-stage kidney disease, cognitive impairment, and circulatory stress [Journal Article; Research Support, Non-U.S. Gov't]. *Hemodialysis International, 23*(3), 356–365. http://doi.org/10.1111/hdi.12754.
15. Eldehni, M. T., & McIntyre, C. W. (2012). Are there neurological consequences of recurrent intradialytic hypotension? [Editorial]. *Semin Dial, 25*(3), 253–256. http://doi.org/10.1111/j.1525-139X.2012.01057.x.
16. Fischl, B. (2012). *FreeSurfer. NEUROIMAGE, 62*(2SI), 774–781. http://doi.org/10.1016/j.neuroimage.2012.01.021.
17. Fischl, B., Salat, D. H., Busa, E., Albert, M., Dieterich, M., Haselgrove, C., van der Kouwe, A., Killiany, R., Kennedy, D., Klaveness, S., Montillo, A., Makris, N., Rosen, B., & Dale, A. M. (2002). Whole brain

segmentation: Automated labeling of neuroanatomical structures in the human brain. *NEURON, 33*(3), 341–355. http://doi.org/10.1016/S0896-6273(02)00569-X.

18. Fischl, B., Sereno, M. I., Tootell, R., & Dale, A. M. (1999). High-resolution intersubject averaging and a coordinate system for the cortical surface. *HUMAN BRAIN MAPPING*, 8(4), 272–284. http://doi.org/10.1002/(SICI)1097-0193(1999)8:4<272::AID-HBM10>3.0.CO;2-4
19. Georgianos, P. I., Pikilidou, M. I., Liakopoulos, V., Balaskas, E. V., & Zebekakis, P. E. (2018). Arterial stiffness in end-stage renal disease-pathogenesis, clinical epidemiology, and therapeutic potentials [Journal Article; Review]. *HYPERTENSION RESEARCH, 41*(5), 309–319. http://doi.org/10.1038/s41440-018-0025-5.
20. Hagmann, P., Cammoun, L., Gigandet, X., Meuli, R., Honey, C. J., Wedeen, V. J., & Sporns, O. (2008). Mapping the structural core of human cerebral cortex [Journal Article; Research Support, N.I.H., Extramural; Research Support, Non-U.S. Gov't]. PLOS BIOLOGY, 6(7), e159. http://doi.org/10.1371/journal.pbio.0060159.
21. Huang, H., & Ding, M. (2016). Linking Functional Connectivity and Structural Connectivity Quantitatively: A Comparison of Methods. *BRAIN CONNECTIVITY, 6*(2), 99–108. http://doi.org/10.1089/brain.2015.0382.
22. Jenkinson, M., Beckmann, C. F., Behrens, T. E., Woolrich, M. W., & Smith, S. M. (2012). *FSL. NEUROIMAGE, 62*(2SI), 782–790. http://doi.org/10.1016/j.neuroimage.2011.09.015.
23. Krishnan, A. V., & Kiernan, M. C. (2009). Neurological complications of chronic kidney disease [Journal Article; Research Support, Non-U.S. Gov't; Review]. *Nature Reviews Neurology, 5*(10), 542–551. http://doi.org/10.1038/nrneurol.2009.138.
24. Kurella, T. M., Xie, D., Yaffe, K., Cohen, D. L., Teal, V., Kasner, S. E., Messé, S. R., Sehgal, A. R., Kusek, J., DeSalvo, K. B., Cornish-Zirker, D., Cohan, J., Seliger, S. L., Chertow, G. M., & Go, A. S. (2011). Vascular risk factors and cognitive impairment in chronic kidney disease: the Chronic Renal Insufficiency Cohort (CRIC) study [Journal Article; Multicenter Study; Research Support, N.I.H., Extramural]. *Clin J Am Soc Nephrol, 6*(2), 248–256. http://doi.org/10.2215/CJN.02660310.
25. Liu, C., Shi, L., Zhu, W., Yang, S., Sun, P., Qin, Y., Tang, X., Zhang, S., Yao, Y., Wang, Z., Zhu, W., & Wang, D. (2020). Fiber Connectivity Density in Cerebral Small-Vessel Disease Patients With Mild Cognitive Impairment and Cerebral Small-Vessel Disease Patients With Normal Cognition. Frontiers in Neuroscience, 14(83) http://doi.org/10.3389/fnins.2020.00083.
26. Liu, K., Zhang, T., Chu, W. C. W., Mok, V. C. T., Wang, D., & Shi, L. (2017). GROUP COMPARISON OF CORTICAL FIBER CONNECTIVITY MAP: AN APPLICATION BETWEEN POST-STROKE PATIENTS AND HEALTHY SUBJECTS. NEUROSCIENCE, 344, 15–24. http://doi.org/10.1016/j.neuroscience.2016.12.026.
27. Liu, K., Zhang, T., Zhang, Q., Sun, Y., Wu, J., Lei, Y., Chu, W. C. W., Mok, V. C. T., Wang, D., & Shi, L. (2016). Characterization of the Fiber Connectivity Profile of the Cerebral Cortex in Schizotypal Personality Disorder: A Pilot Study. Frontiers in Psychology, 7(809) http://doi.org/10.3389/fpsyg.2016.00809.

28. Lourida, I., Thompson-Coon, J., Dickens, C. M., Soni, M., Kuźma, E., Kos, K., & Llewellyn, D. J. (2015). Parathyroid hormone, cognitive function and dementia: a systematic review [Journal Article; Research Support, Non-U.S. Gov't; Review; Systematic Review]. *PLoS One, 10*(5), e127574. http://doi.org/10.1371/journal.pone.0127574.
29. Lu, H., Gu, Z., Xing, W., Han, S., Wu, J., Zhou, H., Ding, J., & Zhang, J. (2019). Alterations of default mode functional connectivity in individuals with end-stage renal disease and mild cognitive impairment [Journal Article]. *BMC Nephrology, 20*(1), 246. http://doi.org/10.1186/s12882-019-1435-6.
30. Ma, X., Jiang, G., Li, S., Wang, J., Zhan, W., Zeng, S., Tian, J., & Xu, Y. (2015). Aberrant functional connectome in neurologically asymptomatic patients with end-stage renal disease [Journal Article; Research Support, Non-U.S. Gov't]. *PLoS One, 10*(3), e121085. http://doi.org/10.1371/journal.pone.0121085.
31. Meunier, D., Fonlupt, P., Saive, A. L., Plailly, J., Ravel, N., & Royet, J. P. (2014). Modular structure of functional networks in olfactory memory [Journal Article; Research Support, Non-U.S. *Gov't]. NEUROIMAGE, 95*, 264–275. http://doi.org/10.1016/j.neuroimage.2014.03.041.
32. Meunier, D., Lambiotte, R., & Bullmore, E. T. (2010). Modular and hierarchically modular organization of brain networks [Journal Article]. *Front Neurosci, 4*, 200. http://doi.org/10.3389/fnins.2010.00200.
33. Mito, R., Raffelt, D., Dhollander, T., Vaughan, D. N., Tournier, J. D., Salvado, O., Brodtmann, A., Rowe, C. C., Villemagne, V. L., & Connelly, A. (2018). Fibre-specific white matter reductions in Alzheimer's disease and mild cognitive impairment [Journal Article; Research Support, Non-U.S. Gov't; Video-Audio Media]. *BRAIN, 141*(3), 888–902. http://doi.org/10.1093/brain/awx355.
34. Mori, S., & van Zijl, P. C. (2002). Fiber tracking: principles and strategies - a technical review [Journal Article; Review]. *NMR IN BIOMEDICINE, 15*(7–8), 468–480. http://doi.org/10.1002/nbm.781.
35. Mu, J., Chen, T., Li, P., Ding, D., Ma, X., Zhang, M., & Liu, J. (2018). Altered white matter microstructure mediates the relationship between hemoglobin levels and cognitive control deficits in end-stage renal disease patients [Journal Article; Research Support, Non-U.S. Gov't]. *HUMAN BRAIN MAPPING, 39*(12), 4766–4775. http://doi.org/10.1002/hbm.24321.
36. Ni, L., Wen, J., Zhang, L. J., Zhu, T., Qi, R., Xu, Q., Liang, X., Zhong, J., Zheng, G., & Lu, G. M. (2014). Aberrant default-mode functional connectivity in patients with end-stage renal disease: a resting-state functional MR imaging study [Journal Article; Research Support, Non-U.S. Gov't]. *RADIOLOGY*, 271(2), 543–552. http://doi.org/10.1148/radiol.13130816.
37. RUSHTON, W. A. (1951). A theory of the effects of fibre size in medullated nerve [Journal Article]. *J Physiol, 115*(1), 101–122. http://doi.org/10.1113/jphysiol.1951.sp004655.
38. Segonne, F., Pacheco, J., & Fischl, B. (2007). Geometrically accurate topology-correction of cortical surfaces using nonseparating loops. *IEEE TRANSACTIONS ON MEDICAL IMAGING, 26*(4), 518–529. http://doi.org/10.1109/TMI.2006.887364.
39. Yamamoto, Y., Ohara, T., Nagakane, Y., Tanaka, E., Morii, F., Koizumi, T., & Akiguchi, I. (2011). Chronic kidney disease, 24-h blood pressure and small vessel diseases are independently associated with

cognitive impairment in lacunar infarct patients [Journal Article]. *HYPERTENSION RESEARCH, 34*(12), 1276–1282. http://doi.org/10.1038/hr.2011.118.

40. Yeh, F., Verstynen, T. D., Wang, Y., Fernandez-Miranda, J. C., & Tseng, W. I. (2013). Deterministic Diffusion Fiber Tracking Improved by Quantitative Anisotropy. *PLoS One, 8*, e8071311. http://doi.org/10.1371/journal.pone.0080713.
41. Yeh, F., Wedeen, V. J., & Tseng, W. I. (2010). Generalized q-Sampling Imaging. *IEEE TRANSACTIONS ON MEDICAL IMAGING, 29*(9), 1626–1635. http://doi.org/10.1109/TMI.2010.2045126.
42. Yeh, F., & Tseng, W. I. (2011). NTU-90: A high angular resolution brain atlas constructed by q-space diffeomorphic reconstruction. *NEUROIMAGE, 58*(1), 91–99. http://doi.org/10.1016/j.neuroimage.2011.06.021.
43. Yin, Y., Li, M., Li, C., Ma, X., Yan, J., Wang, T., Fu, S., Hua, K., Wu, Y., Zhan, W., & Jiang, G. (2018). Reduced White Matter Integrity With Cognitive Impairments in End Stage Renal Disease [Journal Article]. *Frontiers in Psychiatry, 9*, 143. http://doi.org/10.3389/fpsyt.2018.00143.
44. Zalesky, A., Fornito, A., Seal, M. L., Cocchi, L., Westin, C. F., Bullmore, E. T., Egan, G. F., & Pantelis, C. (2011). Disrupted axonal fiber connectivity in schizophrenia [Journal Article; Research Support, N.I.H., Extramural; Research Support, Non-U.S. Gov't]. *Biol Psychiatry, 69*(1), 80–89. http://doi.org/10.1016/j.biopsych.2010.08.022.
45. Zheng, G., Wen, J., Zhang, L., Zhong, J., Liang, X., Ke, W., Kong, X., Zhao, T., He, Y., Zuo, X., Luo, S., Zhang, L. J., & Lu, G. M. (2014). Altered brain functional connectivity in hemodialysis patients with end-stage renal disease: a resting-state functional MR imaging study [Journal Article; Research Support, Non-U.S. Gov't]. *METABOLIC BRAIN DISEASE, 29*(3), 777–786. http://doi.org/10.1007/s11011-014-9568-6.

Figures

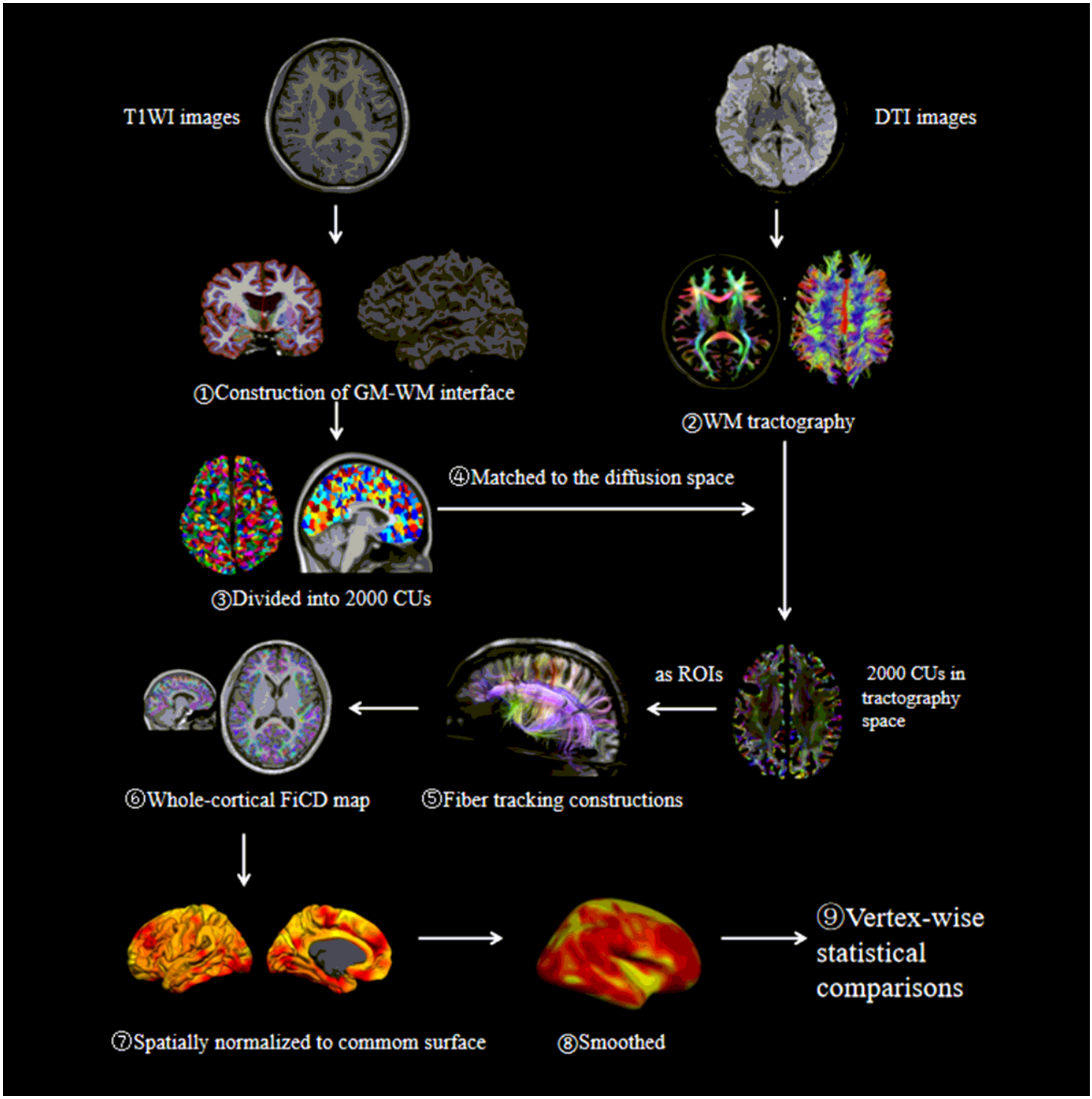

Figure 1

The overall workflow of FiCD mapping pipeline. First, the cortical GM–WM interface is extracted from high spatial resolution T1-weighted images. Second, WM tractography are constructed using DTI imaging. Third, the GM–WM interface is parcellated into 2000 CUs. Fourth, the CUs are transformed into the tractography space. Five, the CUs are used as ROIs to select association fibers. Six, FiCD value is calculated for each CU and a whole-cortex FiCD map is generated. Seven, the map is spatially normalized to common brain surface. Finally, after Gaussian smoothing, the FiCD map is ready for group-level

comparisons. (FiCD: fiber connectivity density; GM: gray matter; WM: white matter; CUs: cortical units; ROI: regions of interest.)

Figure 2

Between-group comparison of ESRD patients vs. HCs. Left panel: Compared with HCs, the FiCD values of the bilateral DLPFC (including the bilateral middle and inferior frontal gyrus), inferior parietal, lateral middle temporal, and right middle occipital cortex were significantly decreased (blue) in ESRD patients, while some regions in the bilateral DLPFC (including the bilateral middle and right inferior frontal gyrus), lateral temporal (including the bilateral superior and right middle temporal gyrus), and left middle occipital cortex of ESRD patients showed significantly increased (red) FiCD values ($P < 0.01$ with Monte Carlo correction). Right panel: The mean global FiCD value was significantly decreased in ESRD patients compared with HCs ($p<0.05$). (ESRD: end-stage renal disease; HCs: health controls; FiCD: fiber connectivity density; DLPFC: dorsolateral prefrontal cortex.)

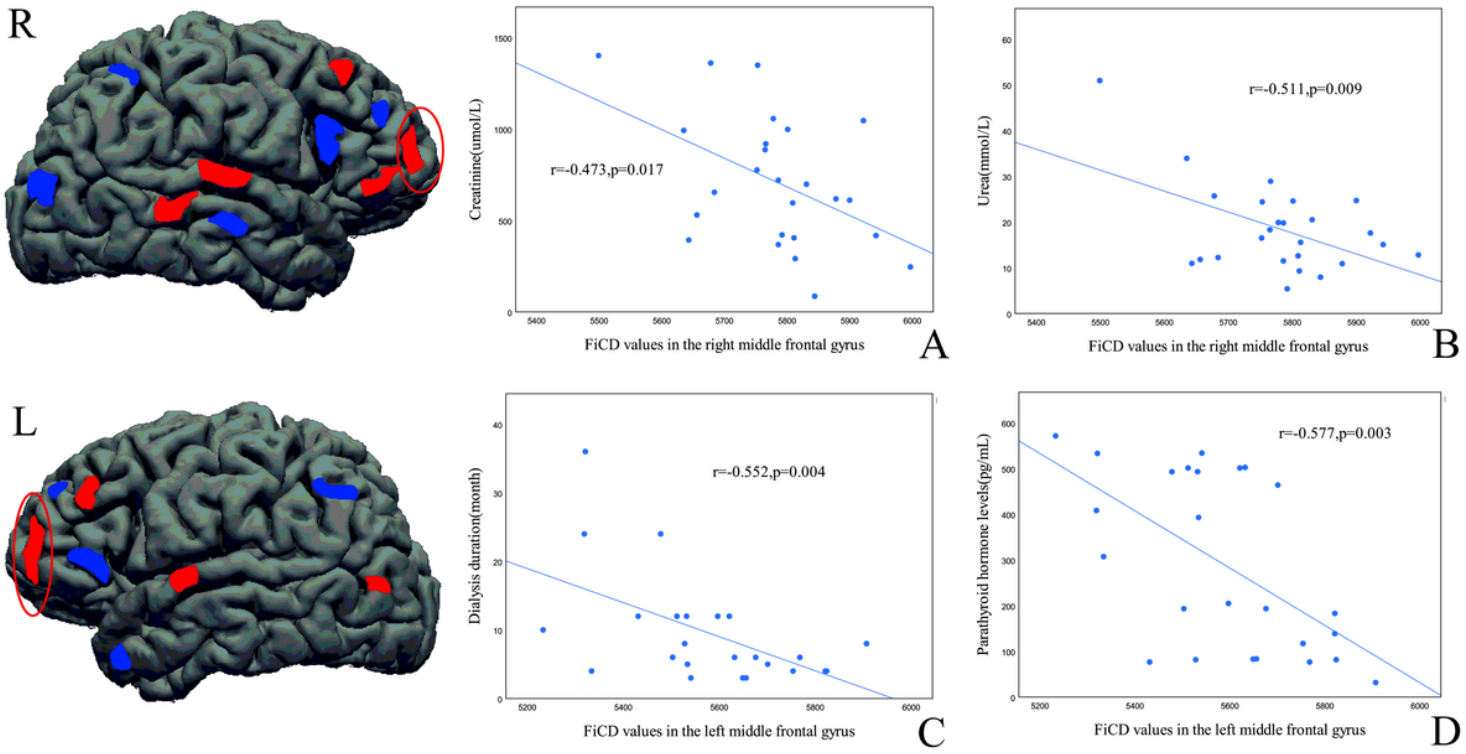

Figure 3

Scatter plot of the relationship between altered FiCD and clinical variables in ESRD patients. The increased FiCD values in the right middle frontal gyrus were negatively correlated with serum creatinine(A) and urea levels(B). And the increased FiCD values in the left middle frontal gyrus were negatively correlated with dialysis duration(C) and PTH levels(D). (FiCD: fiber connectivity density; ESRD: end-stage renal disease; PTH: parathyroid hormone.)

Supplementary Files

This is a list of supplementary files associated with this preprint. Click to download.

- authorchecklist.pdf